Analytical Methods

Accepted Manuscript

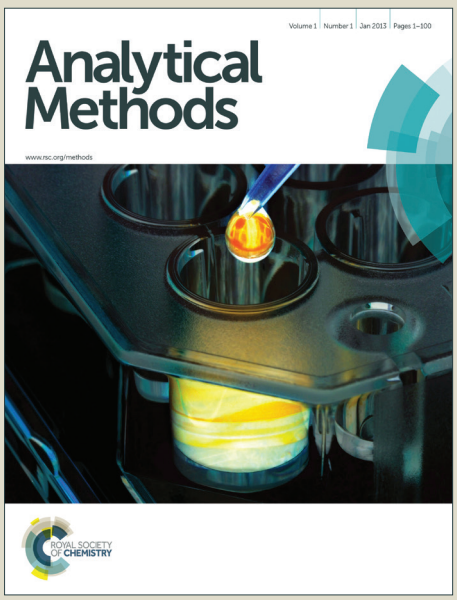

ROYAL SOCIETY OF CHEMISTRY

www.rsc.org/methods

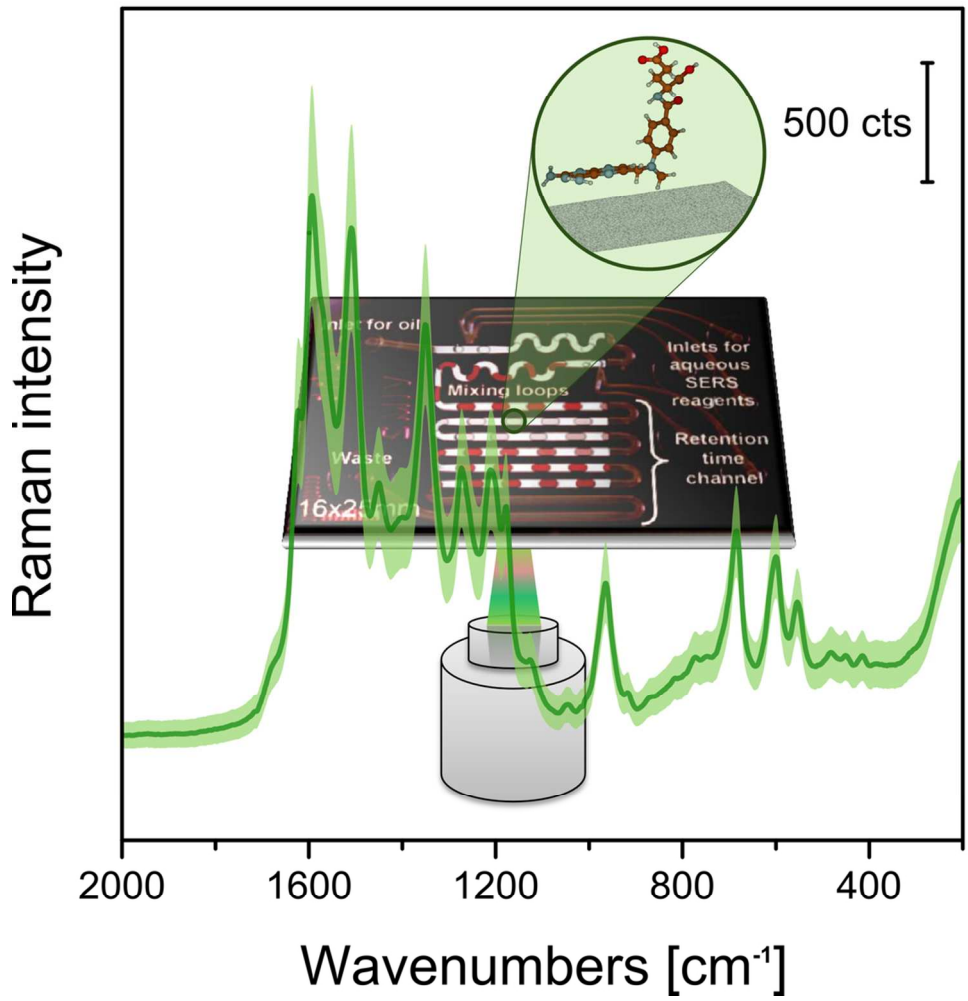

Methotrexate (MTX), an antifolate antibiotic, is detected in a lab-on-a-chip device via surface enhanced Raman spectroscopy (LOC-SERS) in the therapeutic range of 10 μM to 0.1 μM.
100x99mm (300 x 300 DPI)

Journal Name

RSCPublishing

ARTICLE

LOC-SERS: towards point-of-care diagnostic of Methotrexate

Cite this: DOI: 10.1039/xoxxoooooox

I. J. Hidi,[a*] A. Mühlig, [a*] M. Jahn, [a] F. Liebold, [b] D. Cialla,[a,c] K. Weber [a,c] and J. Popp [a,c] ,

Received ooth January 2012,
Accepted ooth January 2012

DOI: 10.1039/xoxxoooooox

www.rsc.org/

Therapeutic drug monitoring is of major importance in case of medication with narrow therapeutic range as well as when pharmacokinetic/pharmacodynamic variability is suspected. Methotrexate (MTX), an antifolate antibiotic, proved to be toxic regardless the chosen treatment schedule. Within this contribution, a new analytical method was used for the detection of MTX. Linear response was achieved in the 0.2-2 µM concentration range, with a limit of detection ≈ 0.17 µM. The lab-on-a-chip surface enhanced Raman spectroscopy (LOC-SERS) approach combines the fingerprint specificity and high sensitivity of SERS with the high sample throughput of a microfluidic platform. Additionally, it is shown that due to the chemical affinity of the MTX molecules towards Ag nanostructures, the pH value of the solving medium highly affects the obtained SERS signal. More specifically, SERS signals with well resolved bands can be obtained from deprotonated MTX molecules due to the binding to the metallic surface via the amine groups of the aromatic ring.

Introduction

Today's cancer therapy makes it essential to monitor and optimize the concentration of the administered medication in blood or other biological fluids.[1-4] Narrow therapeutic range, variability of the patient's characteristics due to age, physiology and/or disease, are only a few parameters which may strongly influence the pharmacokinetic/pharmacodynamic outcome of a given drug. For example, the antifolate Methotrexate (MTX) (see chemical structure in Fig.1), administered in both low-[5] and high-dosage[6-8] (LD-MTX and HD-MTX) treatment schemes, can exhibit high toxicity, overdosage leading to mortality.[9] Furthermore, the therapeutic range of MTX is in the concentration range of micro molar the exact value being strongly dependent on whether it is administered as a single agent or in combination with other drugs.[10] The plasma MTX concentration at 42 hours after the start of HD-MTX infusion should be ≤ 1.0 µM, high risk toxic adverse effects being associated with concentrations ≥ 10 µM.[6, 11, 12] Therefore, from the clinical point of view concerning HD-MTX, it is essential to detect plasma MTX concentration between 10 µM and 0.1 µM.

In order to prevent unwanted clinical outcome, therapeutic drug monitoring (TDM) is employed in clinical settings. Due to TDM the determination of the effective and, at the same time, safe dosage is possible. The concentration in biological fluids is commonly screened with various techniques, such as: immunoassays,[13, 14] gas or a high pressure distribution chromatographic devices[15-18] and the dosage of the medication is regulated to the optimal therapeutic region by taking into account the patient characteristics.

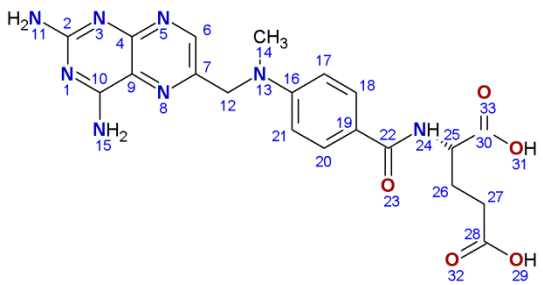

Fig. 1 Chemical structure of MTX.

However, even if chromatographic methods show high specificity and sensitivity, they are time consuming and expensive, they require highly specialized personnel and more than one device in order to assess the drug concentrations. Therefore, the development of a new method with less technical complexity and faster analysing times is needed.

An innovative approach for the point-of-care (POC) diagnostic is the LOC-SERS (lab-on-a-chip surface enhanced Raman spectroscopy) technique.[19-22] Raman spectroscopy offers high specificity providing information concerning the molecular vibrations of the target molecule. As a result, labelling is not required as compared e.g. with fluorescence spectroscopy. However, the intensity of the inelastically scattered light is several orders of magnitude smaller than the excitation and therefore the efficiency is extremely poor. As a

consequence, SERS is more appealing for medical diagnostics.[23-25] It gains its advantage due to a signal amplification effect of up to 8 orders in magnitude.[26] This is a result of the interaction of the analyte molecules with the intense local electromagnetic fields generated at the surface of metallic nanostructures.[26-28] Furthermore, SERS measurements carried out within a microfluidic device with a liquid/liquid segmented flow, where analyte-containing droplets are formed in a carrier fluid like e.g. oil, show great potential for bioanalytics.[19-22] To be more precise, minimal sample amounts are required and only short analysis times are needed, leading to significant cost reductions.

Within this contribution, results of MTX determination out of aqueous solution by means of LOC-SERS will be presented. To the best of our knowledge, this is the first study to prove that SERS offers the possibility of detecting MTX in the target therapeutic concentration range (2 µM to 0.2 µM).

Materials and Methods

Chemicals and reagents

The Methotrexate hydrate powder used during measurements was purchased from Sigma Aldrich and meets the U.S. Pharmacopeial Convention testing specifications. Other reagents, such as mineral oil used for the realization of segmented flow profile, KOH and KCl, HCl, as well as silver nitrate and sodium citrate were of analytical grade and were also purchased from the same provider.

Sample preparation

Due to the low water solubility of MTX, solutions with different pH value were prepared for preliminary tests. A first solution of pH 10 was prepared by solving the MTX powder in a KOH solution of 1 mM concentration. For achieving pH 12 a 150 mM KOH solution was used. Finally, by adding HCl (1 M) to the last solution, pH 2 was achieved.

For LOC-SERS measurements the 150mM KOH solution was chosen. Stock solution of 1mM MTX was prepared and further diluted in order to obtain the desired concentrations (10^{-4}, 10^{-5} and 10^{-6} M).

The Ag colloid was prepared by reducing silver nitrate with sodium citrate according to the Lee-Meisel protocol.[29] Transmission and scanning electron micrograph of this type of nanoparticles can be found elsewhere.[27, 30, 31]

Instrumentation

Extinction spectra of the as prepared colloidal suspension, of MTX, as well as of different mixtures (i.e. colloid:buffer with pH 2, 10 and 12, colloid:MTX) were recorded with a Jasco V650 diode-array spectrophotometer in the wavelength range of 850–230 nm.

The reference Raman spectrum of the target analyte was recorded using as excitation a 785 nm laser line of a commercially available WITec Raman microscope (WITec GmbH, Ulm, Germany). The average power at the sample surface was 80 mW and 10 accumulated spectra of 5 s integration time were acquired.

Before the actual LOC-SERS measurements, preliminary tests were performed in order to assess the optimal measurement conditions. Therefore, for every measurement equal amounts of colloid and buffer/analyte solutions were mixed and finally 1 M KCl was added for inducing the aggregation of nanoparticles (mixing ratio: 1:1:0.1). The mixtures were pipetted in quartz cuvettes. For spectra acquisition, a commercially available WITec Raman microscope (WITec GmbH, Ulm, Germany) with an Ar^+ laser (514 nm) and 2 mW incident laser power at the sample surface was used. The same objective (Nikon 20x, N.A. 0.4) was employed for focusing the laser as well as for collecting the backscattered light. For acquisition 10 accumulated spectra of 5s integration time were recorded.

For LOC-SERS measurements a 16x25 mm^2 sized all-glass microfluidic chip with six inlet ports to add the reagents was employed (Scheme 1). A more detailed description can be found elsewhere.[32, 33] The aqueous droplet segments were generated with the MTX and the 150mM KOH solution at the first dosing unit. The citrate reduced Ag colloid and its activation agent, 1M potassium chloride, was injected into these segments via a second dosing unit. The reproducible addition of analytes is provided by a computer controlled neMESYS Cetoni high performance syringe pump system. During measurements, the applied flow rates were fixed for the carrier medium mineral oil (0.01 µl/s), for the colloidal solution (0.009 µl/s) and the potassium chloride (0.001 µl/s). In order to obtain different concentrations of the analyte, the flow rates of the analyte solution (0, 0.002351, 0.004703, 0.0093, 0.014 µl/s) and mixing 150mM KOH (0.014, 0.01165, 0.0093, 0.0047, 0 µl/s) were changed. Therefore, dilutions occurred within the droplet created at the first dosing unit by mixing MTX solution with the 150mM KOH medium. This resulted in the following in droplet concentrations of the analyte before mixing in colloid and KCl: $1{,}68 \cdot 10^{-x}$ M, $3{,}36 \cdot 10^{-x}$ M, $6{,}65 \cdot 10^{-x}$ M and $1{,}00 \cdot 10^{-(x-1)}$ M, where x=5, 6, 7.

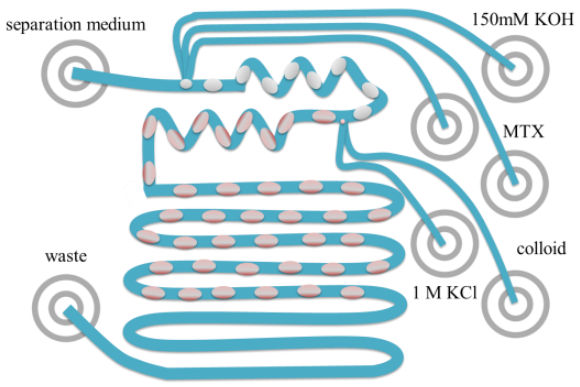

Scheme 1 LOC-SERS device.

In order to get optimal results, the microfluidic chip was mounted on the microscope table of a HR 800 LabRam

spectrometer (Horiba Jobin-Yvon). The frequency doubled Nd:YAG laser (excitation wavelength 532 nm) was focused into the micro channel of the microfluidic chip through an inverse microscope (Olympus IX 71 with Olympus 20x UPlan FLN objective). The backscattered SERS signal was collected through the same objective. During measurements a 300 lines/mm grating (resolution ca. 10 cm^{-1}) and a back-illuminated CCD camera (1024 x 512 pixels) were employed. Spectra were recorded continuously with integration times of 1s during continuous flow. The power at the samples surface was 10 mW; higher laser power being necessary, as compared with the cuvette measurements, due to the dynamic flow. The time needed in order for an aqueous and an oil phase to pass through the laser spot is around 8 s. Therefore, alternating SERS spectra of analyte containing droplets, spectra of the oil phase or spectra with contribution from both phases is recorded.[34] The oil spectra are further used for wavelength calibration of the subsequent SERS spectra.

Results and Discussions

UV-Vis absorption characteristics

According to the absorption profile of the prepared silver colloids, the plasmon resonances are located at ~ 425 nm. As a result of the addition of 150mM KOH solution (pH 12) as well as 1M HCl (pH 2) the absorption band is broadened. This is a consequence of the aggregation of the Ag nanoparticles.

Concerning MTX, its extinction profile shows three absorption peaks. This is due to the strong $\pi \rightarrow \pi^*$ and $\sigma \rightarrow \sigma^*$ electronic transitions.[35] The bands located at 257 and 372 nm are due to the pteridine group, the first one is ascribed to the $1L_a$ while the second one to the $1L_b$ transition. The 308 nm absorption is due to the p-amino benzoyglutamic moiety.[36, 37] When the colloidal solution and the analyte are mixed a broadening of the 372 nm band occurs due to the contribution of the plasmon resonances.

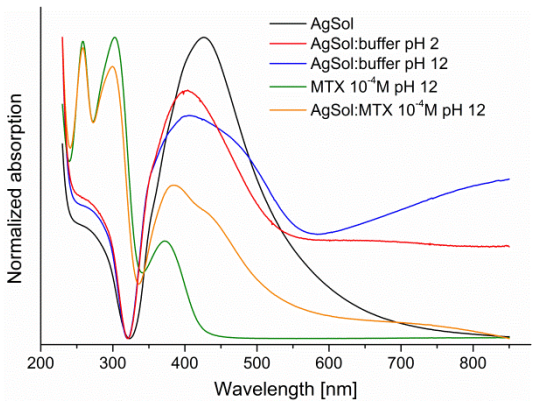

Fig. 2 UV-Vis absorption spectra of the Ag colloid (black); Ag colloid:buffer with pH 2 (red); Ag colloid:buffer with pH 12 (blue); (MTX/pH 12) 10^{-4}M (green) and Ag colloid:(MTX/pH 12) 10^{-4}M (orange) solutions.

Cuvette based SERS measurements

The reference spectrum of the MTX powder (Fig. 3) presents multiple bands, the vibrational analysis being previously presented by Ayyappan et.al.[35] Compered to this, the SERS signal of the MTX solution with pH 12 is slightly different. This may be caused by the deprotonation induced by the addition of KOH molecules. The deprotonation may occur at the O29 and/or at the O31 site (see Fig.1) due to the acidic activity of the carboxyl (COOH) group.

An additional explanation could be given by considering that the orientation of the molecule at the metallic nanoparticle's surface also plays an important role. It is well known, that vibrational modes perpendicular to the surface are significantly enhanced when compared to the ones parallel to it.[38-40] Furthermore, generally, the bonding of molecules to the silver surface can happen either through the lone pair electrons of the nitrogen or oxygen atoms.[41]

In the case of the deprotonated MTX, the attachment to the Ag nanoparticles could be via the amino groups. This is confirmed by the shift of the 1327 cm^{-1} band, ascribed to the NH_2 deformation, by 19 cm^{-1}.

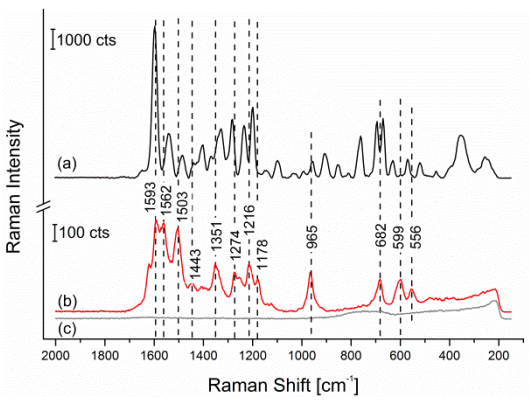

Fig. 3 Reference Raman spectrum measured on powder MTX @785 nm (a); SERS spectra of MTX 0.4 mM pH 12 (b) and background signal (c) of the colloid mixed with 150 mM KOH and 1M KCl (1:1:0.1) @514nm.

Additionally, the pteridine ring is oriented parallel to the metallic surface suggested by the disappearance of the 1403 cm^{-1} band assigned to C=N vibration (see inset Fig.4). Thus, when compared with the Raman spectrum, the ring breathing mode of the aromatic ring at 965 cm^{-1} is strongly enhanced.

Concerning the similarities between the two spectra under discussion, one could argue that several bands of the SERS signal are in good accordance with the ones of the reference. More exactly, in the 1600-1300 cm^{-1} wavenumber region the 1593 cm^{-1} band can be ascribed to the scissoring of the NH_2 group while the one located at 1351 cm^{-1} to the CH_2 scissoring vibrations. Furthermore, in the 1300-900 cm^{-1} spectral region the CH_2 wagging and C-NH_2 vibrations give rise to bands located at 1178 and 1216 cm^{-1}, respectively.

As already mentioned, SERS spectra were acquired for MTX solutions with different pH values. In Fig. 4 the SERS spectra of the MTX solutions with different pH values are presented. In an acidic environment the spectra has a small number of poorly resolved bands. As the result of HCl addition,

protonation of the amine groups at the $N15H_2$ as well as $N11H_2$ affects the chemical affinity of the target molecule towards the metallic surface. Therefore, the number of MTX molecules at the metallic surface is low, leading to a poor SERS signal.

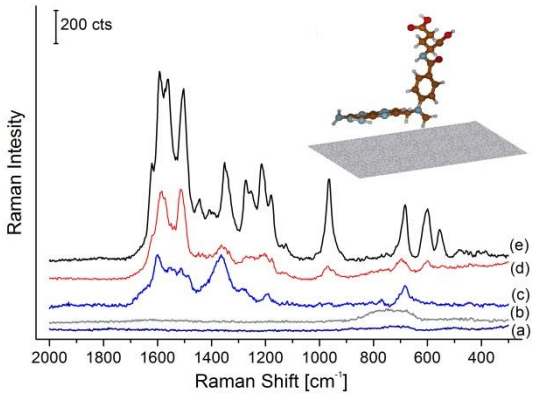

Fig. 4 SERS spectra of the pH adjusted MTX solutions (0.4mM): colloid:buffer with pH 2:KCl (a); colloid:buffer with pH 12:KCl (b); colloid:(MTX/pH 2):KCl (c), colloid:(MTX/pH 10):KCl (d) and colloid:(MTX/pH 12):KCl (e). In the inset: orientation of the MTX molecule on the metal surface.

For alkaline conditions, with increasing the pH from 10 to 12 the Raman signal is significantly improved. This may be due to the better steric orientation of the nitrogen atoms N11 and/or N15 to the metallic surface. As the number of deprotonated MTX molecules gets higher the number of Ag-N bindings increases, leading to the increment of the SERS signal.

Concerning the future experiments for detecting the target analyte out of biological fluids, pH adjustment will be possible by adding a buffer via one of the ports of the microfluidic chip. More exactly, in the case of blood plasma the starting pH value is slightly basic (~7.4). Based on pre-experiments, a buffer will be defined in order to reach an in-droplet pH value of 12.

LOC-SERS measurements

In order to obtain different droplet concentrations of the target analyte a flow profile was employed in the microfluidic channel. Three stem solutions of 10^{-4}, 10^{-5} and 10^{-6} M concentration were injected in order to assess the limit of detection (LOD). As mentioned before, due to the mixing of the MTX solution with the solvent within the droplet formed at the first dosing port the measured concentrations are between 0.16 µM and 93 µM. In Fig. 5 one can see the plot of the mean spectra and their double standard deviation of selected concentration steps. Intermediate concentrations are not shown for the sake of clarity. According to this, spectral features characteristic to MTX are still present at a concentration of 0.17µM.

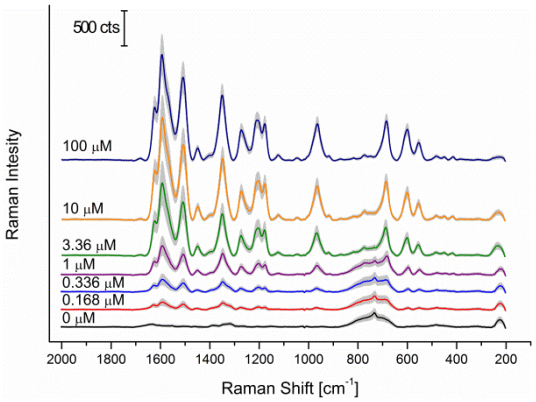

Fig.5 Concentration dependency of the SERS signal of MTX measured by LOC-SERS.

For a better visualisation, the Lorentz fitted peak area of the 965 cm^{-1} band was plotted against the in droplet concentration of MTX (see Fig. 6). Therefore, one may observe, that a linear dependency exists in the 0.2 - 2 µM region, with an LOD ~ 0.17 µM. This concentration domain is useful for the clinical practice when HD-MTX treatments are aimed. For concentrations higher than 10 µM the signal reaches saturation. This may be due to the fact that the surface of the Ag colloids is limited. Therefore, the increment of the number of MTX molecules does not lead to higher signal intensities.

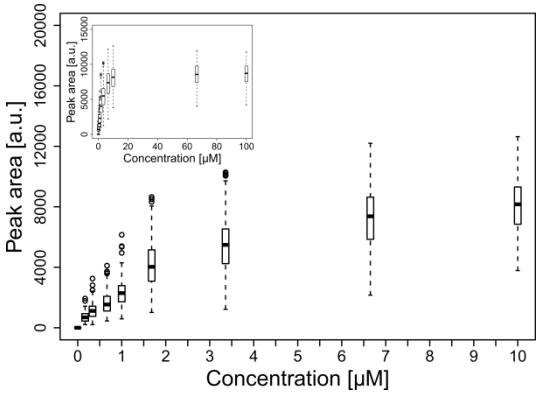

Fig.6 Lorentz fitted peak area of the 965 cm^{-1} band against in droplet concentration of the MTX.

Conclusions

Within this study it was shown that when MTX is solved in a 150 mM KOH solution the deprotonated molecules bind to the silver nanoparticles via amine groups with the pteridine ring oriented parallel to the surface. Additionally, the pH value of the MTX solution has a strong influence on the chemical affinity of the target molecules towards the silver surface. SERS spectra with well resolved bands could be recorded when the solvent had an alkaline character. Furthermore, it was proven that LOC-SERS technology is a promising technique for the detection of biologically relevant molecules in the target therapeutic range. More exactly, in the case of MTX concentrations down to 0.17 µM were detected. Additionally,

the Raman signal vs. MTX concentration showed linearity in the 0.2-2 µM window, concentration range relevant for HD-MTX treatment schedules.

Acknowledgements

The funding of the PhD project of I.J. Hidi within the framework "Carl-Zeiss-Strukturmaßnahme" is gratefully acknowledged. The projects "QuantiSERS" and "Jenaer Biochip Initiative 2.0" within the framework "InnoProfile Transfer – Unternehmen Region" are supported by the Federal Ministry of Education and Research, Germany (BMBF). We thank the microfluidic group of the IPHT for providing the lab-on-a-chip devices for the measurements. Additionally, the help of Konstanze Olschewskithe with the data processing is gratefully acknowledged.

Notes and references

[a] Friedrich Schiller University Jena, Institute of Physical Chemistry and Abbe Center of Photonics, Helmholtzweg 4, 07745 Jena, Germany.

* equally contributed.

[b] Analytik Jena AG, Konrad-Zuse-Straße 1, 07745 Jena.

[c] Leibniz-Institute of Photonic Technology Jena, Albert-Einstein-Str. 9, 07745 Jena, Germany.

1. V. Escudero-Ortiz, J. J. Pérez-Ruixo and B. Valenzuela, *Therapeutic Drug Monitoring*, 2013, 35, 796-802 710.1097/FTD.1090b1013e3182959080.
2. D. J. Cline, H. Zhang, G. D. Lundell, R. L. Harney, H. K. Riaz, J. Jarrah, Y. Li, M. Miyazaki, J. B. Courtney, I. Baburina and S. J. Salamone, *Therapeutic Drug Monitoring*, 2013, 35, 809-815 810.1097/FTD.1090b1013e318296be318201.
3. R. E. Aarnoutse, J. M. Schapiro, C. A. Boucher, Y. A. Hekster and D. M. Burger, *Drugs*, 2003, 63, 741-753.
4. G. L. Owens, K. Gajjar, J. Trevisan, S. W. Fogarty, S. E. Taylor, B. Da Gama-Rose, P. L. Martin-Hirsch and F. L. Martin, *Journal of Biophotonics*, 2013, DOI: 10.1002/jbio.201300157, n/a-n/a.
5. B. N. Cronstein, *Pharmacol Rev*, 2005, 57, 163-172.
6. B. C. Widemann and P. C. Adamson, *The oncologist*, 2006, 11, 694-703.
7. B. L. Asselin, M. Devidas, C. Wang, J. Pullen, M. J. Borowitz, R. Hutchison, S. E. Lipshultz and B. M. Camitta, *Blood*, 2011, 118, 874-883.
8. H. Inaba, R. B. Khan, F. H. Laningham, K. R. Crews, C. H. Pui and N. C. Daw, *Annals of Oncology*, 2008, 19, 178-184.
9. I. Sinicina, B. Mayr, G. Mall and W. Keil, *J Rheumatol*, 2005, 32, 2009-2011.
10. L. Lennard, *Br J Clin Pharmacol.*, 1999, 47, 131-143.
11. K. R. Crews, T. Liu, C. Rodriguez-Galindo, M. Tan, W. H. Meyer, J. C. Panetta, M. P. Link and N. C. Daw, *Cancer*, 2004, 100, 1724-1733.
12. K. R. Crews, Y. Zhou, J. L. Pauley, S. C. Howard, S. Jeha, M. V. Relling and C.-H. Pui, *Cancer*, 2010, 116, 227-232.
13. C. Ritzmo, F. Albertioni, K. Cosic, S. Söderhäll and S. Eksborg, *Therapeutic Drug Monitoring*, 2007, 29, 447-451 410.1097/FTD.1090b1013e318063e318065e318065.
14. S. Marubashi, H. Nagano, S. Kobayashi, H. Eguchi, Y. Takeda, M. Tanemura, K. Umeshita, M. Monden, Y. Doki and M. Mori, *The Journal of Clinical Pharmacology*, 2010, 50, 705-709.
15. E. den Boer, S. G. Heil, B. D. van Zelst, R. J. W. Meesters, B. C. P. Koch, M. L. te Winkel, M. M. van den Heuvel-Eibrink, T. M. Luider and R. de Jonge, *Therapeutic Drug Monitoring*, 2012, 34, 432-439 410.1097/FTD.1090b1013e31825bb31368.
16. C. Sottani, G. Poggi, F. Melchiorre, B. Montagna and C. Minoia, *Journal of Chromatography B*, 2013, 915–916, 71-78.
17. S. Belz, C. Frickel, C. Wolfrom, H. Nau and G. Henze, *Journal of Chromatography B: Biomedical Sciences and Applications*, 1994, 661, 109-118.
18. R. J. W. Meesters, E. den Boer, R. A. A. Mathot, R. de Jonge, R. J. van Klaveren, J. Lindemans and T. M. Luider, *Bioanalysis*, 2011, 3, 1369-1378.
19. A. Walter, A. Marz, W. Schumacher, P. Rosch and J. Popp, *Lab on a chip*, 2011, 11, 1013-1021.
20. A. Marz, B. Monch, P. Rosch, M. Kiehntopf, T. Henkel and J. Popp, *Anal Bioanal Chem*, 2011, 400, 2755-2761.
21. A. Pallaoro, M. R. Hoonejani, G. B. Braun, C. Meinhart and M. Moskovits, *NANOP*, 2013, 7, 073092-073092.
22. X. Lu, D. R. Samuelson, Y. Xu, H. Zhang, S. Wang, B. A. Rasco, J. Xu and M. E. Konkel, *Analytical chemistry*, 2013, 85, 2320-2327.
23. M. Salehi, D. Steinigeweg, P. Ströbel, A. Marx, J. Packeisen and S. Schlücker, *Journal of Biophotonics*, 2013, 6, 785-792.
24. U. S. Dinish, G. Balasundaram, Y. T. Chang and M. Olivo, *Journal of Biophotonics*, 2013, DOI: 10.1002/jbio.201300084, n/a-n/a.
25. P. Negri and R. A. Dluhy, *Journal of Biophotonics*, 2013, 6, 20-35.
26. E. C. Le Ru and P. G. Etchegoin, in *Principles of Surface-Enhanced Raman Spectroscopy*, eds. E. C. L. Ru and P. G. Etchegoin, Elsevier, Amsterdam, 2009, DOI: http://dx.doi.org/10.1016/B978-0-444-52779-0.00010-6, pp. 185-264.
27. D. Cialla, A. März, R. Böhme, F. Theil, K. Weber, M. Schmitt and J. Popp, *Analytical and Bioanalytical Chemistry*, 2012, 403, 27-54.
28. E. C. Le Ru, S. A. Meyer, C. Artur, P. G. Etchegoin, J. Grand, P. Lang and F. Maurel, *Chemical Communications*, 2011, 47, 3903-3905.
29. P. C. Lee and D. Meisel, *The Journal of Physical Chemistry*, 1982, 86, 3391-3395.
30. D. Steinigeweg and S. Schlucker, *Chemical Communications*, 2012, 48, 8682-8684.
31. C. De Bleye, E. Dumont, E. Rozet, P. Y. Sacré, P. F. Chavez, L. Netchacovitch, G. Piel, P. Hubert and E. Ziemons, *Talanta*, 2013, 116, 899-905.
32. T. Henkel, T. Bermig, M. Kielpinski, A. Grodrian, J. Metze and J. M. Köhler, *Chemical Engineering Journal*, 2004, 101, 439-445.
33. A. Marz, K. R. Ackermann, D. Malsch, T. Bocklitz, T. Henkel and J. Popp, *J Biophotonics*, 2009, 2, 232-242.
34. A. März, T. Bocklitz and J. Popp, *Analytical chemistry*, 2011, 83, 8337-8340.

35. S. Ayyappan, N. Sundaraganesan, V. Aroulmoji, E. Murano and S. Sebastian, *Spectrochimica Acta Part A: Molecular and Biomolecular Spectroscopy*, 2010, 77, 264-275.
36. G. Seng, J. Bolard, L. Chinsky and P. Y. Turpin, *Journal of Raman Spectroscopy*, 1982, 13, 100-102.
37. Y. Ozaki, R. W. King and P. R. Carey, *Biochemistry*, 1981, 20, 3219-3225.
38. J. E. Pemberton, M. A. Bryant, R. L. Sobocinski and S. L. Joa, *The Journal of Physical Chemistry*, 1992, 96, 3776-3782.
39. X. Gao, J. P. Davies and M. J. Weaver, *The Journal of Physical Chemistry*, 1990, 94, 6858-6864.
40. H. Grabhorn and A. Otto, *Vacuum*, 1990, 41, 473-475.
41. M. Baia, L. Baia, W. Kiefer and J. Popp, *The Journal of Physical Chemistry B*, 2004, 108, 17491-17496.